0026-895X/11/7903-520–532$20.00
MOLECULAR PHARMACOLOGY
Copyright © 2011 The American Society for Pharmacology and Experimental Therapeutics
Mol Pharmacol 79:520–532, 2011

Vol. 79, No. 3
69039/3669526
Printed in U.S.A.

Site-Directed Mutations near Transmembrane Domain 1 Alter Conformation and Function of Norepinephrine and Dopamine Transporters

Bipasha Guptaroy, Rheaclare Fraser, Aalisha Desai, Minjia Zhang, and Margaret E. Gnegy

Department of Pharmacology, University of Michigan, Ann Arbor, Michigan

Received September 23, 2010; accepted December 13, 2010

ABSTRACT

The human dopamine and norepinephrine transporters (hDAT and hNET, respectively) control neurotransmitter levels within the synaptic cleft and are the site of action for amphetamine (AMPH) and cocaine. We investigated the role of a threonine residue within the highly conserved and putative phosphorylation sequence RETW, located just before transmembrane domain 1, in regulating hNET and hDAT function. The Thr residue was mutated to either alanine or aspartate. Similar to the inward facing T62D-hDAT, T58D-hNET demonstrated reduced [^{3}H]DA uptake but enhanced basal DA efflux compared with hNET with no further effect of AMPH. The mutations had profound effects on substrate function and binding. The potency of substrates to inhibit [^{3}H]DA uptake and compete with radioligand binding was increased in T→A and/or T→D mutants. Substrates, but not inhibitors, demonstrated temperature-sensitive effects of binding. Neither the functional nor the binding potency for hNET blockers was altered from wild type in hNET mutants. There was, however, a significant reduction in potency for cocaine and benztropine to inhibit [^{3}H]DA uptake in T62D-hDAT compared with hDAT. The potency of these drugs to inhibit [^{3}H](−)-2-β-carbomethoxy-3-β-(4-fluorophenyl)tropane-1,5-napthalenedisulfonate (WIN35,428) binding was not increased, demonstrating a discordance between functional and binding site effects. Taken together, these results concur with the notion that the T→D mutation in RETW alters the preferred conformation of both hNET and hDAT to favor one that is more inward facing. Although substrate activity and binding are primarily altered in this conformation, the function of inhibitors with distinct structural characteristics may also be affected.

Introduction

The availability of the monoamine neurotransmitters dopamine (DA) and norepinephrine (NE) around the synaptic cleft is regulated by DA and NE transporters (DAT and NET, respectively), which mediate the reuptake of released neurotransmitter into the presynaptic terminal (Amara and Kuhar, 1993; Giros and Caron, 1993; Blakely and Bauman, 2000). Transporter-mediated reuptake terminates the presence of neurotransmitter at the synaptic cleft.

Both DAT and NET are members of the SLC6 Na^+/Cl^--dependent transporter family (Torres et al., 2003). Substrate transport through these proteins is coupled to the concomitant transport of Na^+ and Cl^- ions (Chen and Reith, 2000; Norregaard and Gether, 2001). An alternating access model was proposed to explain the functioning of these transporters, in which the transporter would oscillate between two primary conformations, an "outward-facing" mode accessible to the extracellular medium and an "inward-facing" mode that is open to the intracellular milieu (Rudnick, 1997). According to this model, both substrate and inhibitors bind the transporter when it assumes an outward-facing conformation. Substrates, however, elicit a conformational change that promotes an inward-facing conformation resulting in translocation of substrate along with Na^+ and Cl^- ions.

Monoamine transporters contain 12 transmembrane domains (TM), connecting intracellular and extracellular loops and intracellular amino and carboxyl termini (Torres et al., 2003). The elucidation of the crystal structure of the bacterial leucine transporter ($LeuT_{Aa}$), a homolog of monoamine transporters, provided insight into the three-dimensional struc-

This work was supported by the National Institutes of Health National Institute on Drug Abuse [Grant DA011697]. This work used the DNA Sequencing Core of the Michigan Diabetes Research and Training Center funded by the National Institutes of Health National Institute of Diabetes and Digestive and Kidney Diseases [Grant DK020572].

Article, publication date, and citation information can be found at http://molpharm.aspetjournals.org.

doi:10.1124/mol.110.069039.

ABBREVIATIONS: DA, dopamine; NE, norepinephrine; DAT, dopamine transporter; NET, norepinephrine transporter; h, human; TM, transmembrane domain; AMPH, amphetamine; KRH, Krebs-Ringer HEPES buffer; GBR12935, 1-[2-(diphenylmethoxy)ethyl]-4-(3-phenylpropyl)-piperazine; WIN35,428, (−)-2-β-carbomethoxy-3-β-(4-fluorophenyl)tropane-1,5-napthalenedisulfonate; ANOVA, analysis of variance; CI, confidence interval; RT, room temperature.

ture of these transporters (Yamashita et al., 2005). The structure revealed a substrate-occluded state possibly representing a state between the outward- and inward-facing conformations and suggested the existence of important ionic interactions among residues in the N terminus (Arg5), TM8 (Asp369), and TM6 (Tyr206) as part of a network of ionic interactions that could constitute an intracellular "gate" (Yamashita et al., 2005; Singh, 2008). Mutagenesis studies demonstrate similar interactions between corresponding residues in DAT (Arg60 in the N terminus, Asp436 at the end of TM8 and Tyr335 in intracellular loop 3 close to TM6) (Kniazeff et al., 2008). These studies establish that the N-terminal Arg60 (DAT) residue, which is highly conserved in monoamine transporters, plays a critical role in transporter function. Mutations of Tyr335 and Asp436 also have profound impact on DAT conformation and function; specifically, mutation of all of these residues (Arg60, Asp436, and Tyr335) of DAT to Ala seems to promote a conformation (presumably inward-facing) of the transporter in which DA uptake is significantly compromised (Loland et al., 2002, 2004; Kniazeff et al., 2008).

The RETW motif is conserved in all monoamine transporters (residues 60–63 in DAT and 56–59 in NET), and mutations within this motif have robust effects on hDAT function. Mutation of both Arg and Trp, but not Glu, within this motif in hDAT profoundly affects DA uptake (Chen et al., 2001; Kniazeff et al., 2008). In the corresponding sequence (RDTW) in GAT-1, deletion of Arg44, Thr46, or Trp47 renders the transporter totally inactive (Bennett et al., 2000), and only certain substitutions are tolerated. We have demonstrated that mutation of the Thr residue within the RETW motif similarly has a profound effect on DAT conformation and function (Guptaroy et al., 2009). Mutation of Thr62 to Asp in DAT resulted in a transporter that favors an inward-facing conformation, which promotes constitutive efflux of DA from cells and prevents accumulation of internal DA. We now present evidence for a similar, although not identical, effect of the same mutations in the corresponding Thr residue (Thr58) in hNET. These studies further establish the importance of the highly conserved N-terminal residues proximal to TM1 in maintaining monoamine transporter conformations that sustain normal transporter function.

Monoamine transporters are also the target for both therapeutic and abused drugs such as antidepressants, AMPH, and cocaine (Norregaard and Gether, 2001). Mutants of DAT with altered conformational equilibrium are useful tools in binding studies and provide invaluable information about the potency of structurally diverse transporter inhibitors (Schmitt et al., 2008; Liang et al., 2009). These studies demonstrate that the transporter and ligand conformation determines the interaction between them. In the present study, we used the N-terminal threonine mutants of hDAT (Thr62) and hNET (Thr58) to investigate the effect of various substrates and inhibitors on transport and binding characteristics. We find that in Thr-to-Asp mutants, which favor an inward-facing conformation, the affinity for both catechol and noncatechol substrates is enhanced and that substrate binding is temperature-dependent. Conversely, these mutations have no appreciable effect on the interaction of the transporters with most inhibitors, with the exception of benztropine and cocaine in hDAT.

Materials and Methods

Mutagenesis and Generation of Stable Cell Lines. The hDAT mutants and cell lines were generated as described previously (Guptaroy et al., 2009). The hNET mutants were generated by polymerase chain reaction using sense and antisense oligonucleotides and pfu polymerase (Stratagene, La Jolla, CA). After digestion of parental DNA with DpnI (Promega Corporation, Madison, WI), competent DH5α cells were transformed with mutagenic DNA. Mutations were confirmed by DNA sequencing, and the cDNAs were used to transfect human embryonic kidney 293 cells using Lipofectamine (Invitrogen, Carlsbad, CA). A stable pool of G418-resistant cells was selected and maintained in the presence of 100 μg/ml G418 in Dulbecco's modified Eagle's medium supplemented with 10% fetal bovine serum and 1% penicillin/streptomycin at 37°C and 5% CO_2.

Surface Biotinylation and Immunoblotting. To label cell-surface transporters, cells were treated with sulfosuccinimidyl-2-(biotinamido) ethyl-1,3-dithiopropionate (sulfo-NHS-SS biotin); Pierce, Rockford, IL) at 4°C as described previously (Johnson et al., 2005). The reaction was quenched for 15 min with 100 mM glycine at 4°C. Cells were lysed in solubilization buffer (25 mM Tris, 150 mM NaCl, 1 mM EDTA, 5 mM *N*-ethylmaleimide, 100 μM phenylmethylsulfonyl fluoride, and 1% Triton X-100) containing protease inhibitors (Roche, Indianapolis, IN) and centrifuged at 20,000*g* to remove cell debris. Biotinylated proteins in cell lysates containing 800 μg of protein were bound to 50 μl of streptavidin beads (Pierce) by incubating for 1 h at room temperature (RT). The beads were washed with solubilization buffer and eluted in 25 μl of SDS-polyacrylamide gel electrophoresis sample buffer containing 100 mM dithiothreitol and resolved by electrophoresis on a 10% Tris-glycine gel along with samples of the lysate. Proteins were transferred to a nitrocellulose membrane (GE Healthcare, Chalfont St. Giles, Buckinghamshire, UK) and blocked for 1 h in 5% milk in 10 mM Tris, pH 7.4, 150 mM NaCl, and 0.1% Tween 20. hNET was detected using anti-NET (Alpha Diagnositcs, San Antonio, TX) and horseradish peroxidase-conjugated secondary antibody (Santa Cruz Biotechnologies Inc., Santa Cruz, CA) by enhanced chemiluminescence reagent (Pierce). Quantification of bands was done by densitometry using Scion Image software (Scion Corporation, Frederick, MD).

[^{3}H]DA Uptake and Competition Assays. Cells were plated on 24-well plates at a density of 10^5 cells per well 1 day before performing the assays. [^{3}H]DA uptake was measured in KRH (25 mM HEPES, pH 7.4, 125 mM NaCl, 4.8 mM KCl, 1.2 mM KH_2PO_4, 1.3 mM $CaCl_2$, 1.2 mM $MgSO_4$, and 5.6 mM glucose containing 50 μM pargyline, 1 mM tropolone, and 50 μM ascorbic acid) in the absence or presence of 10 μM 1-[2-(diphenylmethoxy)ethyl]-4-(3-phenylpropyl)-piperazine (GBR12935; Sigma, St. Louis, MO) or 100 μM cocaine. The initial rate of uptake was analyzed using 30 nM to 3 μM [^{3}H]DA (specific activity, 59.3 Ci/mmol; PerkinElmer Life and Analytical Sciences, Waltham, MA) for 2 min at room temperature in a final volume of 250 μl. The reaction was stopped by rapidly washing three times with 1 ml of ice-cold phosphate-buffered saline. Cells were solubilized in 1% SDS and radioactivity was measured using Scintiverse (Thermo Fisher Scientific, Waltham, MA) in a liquid scintillation counter (LS 5801; Beckman Coulter, Fullerton, CA). For competition assays, cells were incubated with [^{3}H]DA for 3 min in the presence of increasing concentrations of competing substrates or inhibitors (Sigma-Aldrich). Cells were preincubated with inhibitors for 10 min before initiating [^{3}H]DA uptake and substrates were added simultaneously with [^{3}H]DA. Nonspecific binding was determined in the presence of transporter inhibitors (DAT, 5–10 μM GBR12935 or 100 μM cocaine; NET, 1–3 μM desipramine or 100 μM cocaine). The IC_{50} values for uptake inhibition by substrates will represent the K_m for the substrates. In case of the inhibitors, the IC_{50} values are close to the K_i values, because 30 nM [^{3}H]DA is far below the K_m for DA.

[^{3}H]DA Efflux. Basal efflux of [^{3}H]DA was measured in cells plated on 12 well plates at a density of 1.5×10^5 cells per well. Cells

were loaded for 20 min at room temperature with 1 μM [^{3}H]DA in KRH. After loading, cells were washed rapidly with KRH three times. KRH (500 μl) was added and removed after 5 min for scintillation counting, and this was repeated at 10- and 15-min time points. After 15 min, cells were lysed in 1% SDS and counted to determine the amount of [^{3}H]DA remaining in the cells. Cells from a separate well were lysed immediately after loading with [^{3}H]DA to obtain an estimate of the total amount of [^{3}H]DA in the cells at the start of the experiment.

AMPH-Stimulated DA Efflux. Confluent 100-mm plates of cells were washed twice with KRH and incubated at 37°C with 15 μM DA for 30 min. Cells were washed with KRH, harvested, and resuspended in 200 μl of KRH, and 150 μl of the cells were placed on a Whatman GF/B filter (Whatman, Clifton, NJ) in a chamber of a superfusion apparatus (SF-12; Brandel, Gaithersburg, MD). Superfusion chambers were maintained at room temperature, and KRH was perfused at a rate of 400 μl/min. Samples were collected every 2 min. After a 45-min wash to reduce baseline, cells received a 2-min bolus of 10 μM *d*-AMPH. Fractions were collected for the next 50 min. Samples were collected into vials containing 25 μl of an internal standard solution (0.05 M $HClO_4$, 4.55 mM dihydrobenzylamine, 1 M metabisulfate, and 0.1 M EDTA) as described previously (Kantor et al., 2001). Samples were stored at −80°C, and DA content was measured by high-pressure liquid chromatography with electrochemical detection. DA efflux was quantified as the peak DA in the eluent.

Binding Assays. Cells were plated on 24-well plates at a density of 10^5 cells per well 1 day before the experiment. Cells were rinsed with KRH and binding of 4 nM [^{3}H](−)-2-β-carbomethoxy-3-β-(4-fluorophenyl)tropane-1,5-napthalenedisulfonate (WIN35,428) (specific activity, 85 Ci/mmol; PerkinElmer Life and Analytical Sciences) (hDAT) or 3 nM [^{3}H]nisoxetine (specific activity, 87.2 Ci/mmol; PerkinElmer Life and Analytical Sciences) (hNET) was measured in the absence or presence of transporter inhibitors (DAT, 5–10 μM GBR-12935 or 100 μM cocaine; NET, 1–3 μM desipramine or 100 μM cocaine). All assays were performed at the peak time for saturation binding determined previously (30 min for [^{3}H]WIN35,428 and 90 min for [^{3}H]nisoxetine). Reactions were incubated for 30 or 90 min at room temperature or on ice as indicated in the figure legends. Binding was attenuated by rapidly washing three times with ice-cold phosphate-buffered saline. Cells were solubilized in 1% SDS and counted in a Beckman scintillation counter using Scintiverse. In competition assays, the indicated concentrations of substrates or inhibitors were used during incubations. For K_d determination, cells were incubated with increasing concentrations of [^{3}H]WIN35,428 (1–100 nM) for hDAT and [^{3}H]nisoxetine (1–30 nM) for hNET and processed as described above.

Statistical Analysis. Kinetic constants, including K_m, V_{max}, and IC_{50} values for the transporter constructs were determined by nonlinear regression analysis of the mean values for each mutant using Prism version 5 (GraphPad Software, San Diego, CA). Statistical significance was determined using Prism version 5 either by comparison with wild type using a two-way ANOVA with post-test Bonferroni analysis or with an *F* test by comparing fits in which selected values were constrained to be equal or were allowed to differ. The null hypothesis was that the best-fit parameter for the value did not differ. A conclusion of statistical significance represents a rejection of the null hypothesis and indicates a difference between designated values. Values plus the 95% confidence levels are reported. In most cases, the *F* distributions are reported in the tables and figure legends to maintain flow in the text.

Results

Surface Expression and DA Uptake in hNET and Mutant Transporters. Both T58A-hNET and T58D-hNET express in the cell at levels equivalent to that of hNET but traffic less efficiently to the cell surface compared with hNET. As shown in Fig. 1A, total transporter levels in the lysate on a protein basis were the same for all three transporters, but the amount of surface transporter was reduced in T58A-hNET and T58D-hNET (Fig. 1A). A quantitative representation of the amount of surface transporter as a multiple of hNET demonstrated that T58A-hNET is expressed on the surface at 60% and T58D-hDAT at 50% of the level of hNET (Fig. 1B, $n = 7$).

Inward transport through the hNET mutants was determined by measuring [^{3}H]DA uptake. Using [^{3}H]DA is valid because the NET can transport both NE and DA. In fact, NET has greater affinity for DA than NE and greater V_{max} values for DA uptake compared with NE (Gu et al., 1994; Eshleman et al., 1999). In view of this preference of NET for DA, we used [^{3}H]DA transport to understand the properties of substrate transport in the hNET constructs. Other mu-

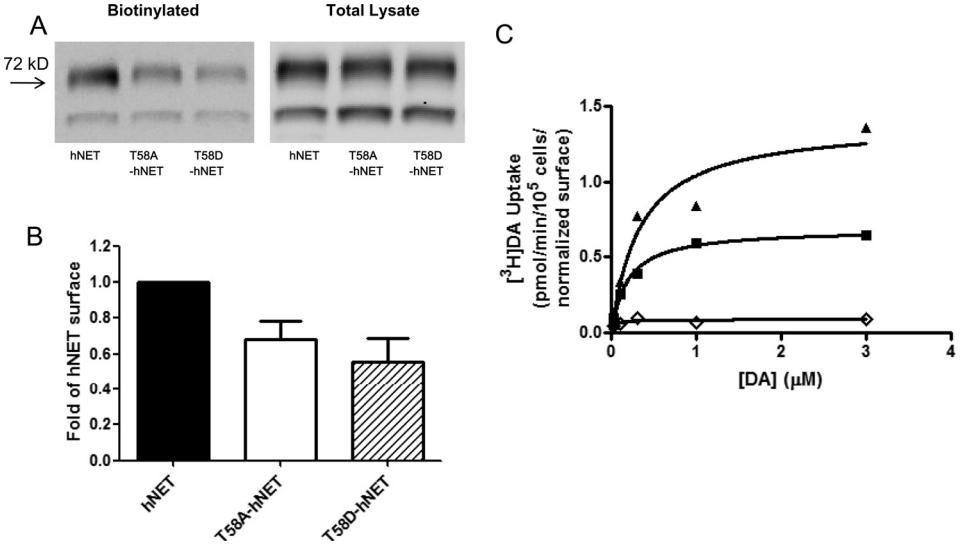

Fig. 1. Surface expression and [^{3}H]DA uptake in hNET and hNET-T58 mutants. Cell surface expression of hNET, T58A-hNET, or T58D-hNET was analyzed by biotinylation as described under *Materials and Methods*. A representative Western blot (A) and quantitation of surface transporter compared with hNET (B) are shown. Data represent mean ± S.E.M, $n = 7$. C, [^{3}H]DA uptake ($n = 3$) was calculated in hNET (■), T58A-hNET (▲), and T58D-hNET (◇) by measuring initial rates at increasing concentrations of [^{3}H]DA as described under *Materials and Methods*.

tants of NET have been characterized on the basis of their DA transport properties (Danek Burgess and Justice, 1999).

[^{3}H]DA uptake velocities for the hNET constructs were determined from the initial rates calculated from time-course curves at varying concentrations of [^{3}H]DA. Values were normalized to surface expression of hNET. The data in Fig. 1C show that T58D-hNET cells had a dramatically reduced V_{max} compared with hNET ($p < 0.05$). There was a similar significant reduction of the V_{max} for [^{3}H]DA uptake in T62D-hDAT compared with hDAT (Table 1) (Guptaroy et al., 2009). On the contrary, there was a significant increase in the normalized (corrected for surface expression) V_{max} value for [^{3}H]DA uptake in T58A-hNET (1.3 pmol/10^5 cells per minute) compared with hNET (0.76 pmol/10^5 cells per minute, $p < 0.0003$). This is in contrast to the corresponding hDAT mutant T62A-hDAT (Guptaroy et al., 2009), in which the V_{max} value was significantly lower than that of hDAT (Table 1). In hNET, therefore, the mutation of Thr58 to Ala or to Asp has opposing effects on [^{3}H]DA uptake. These results demonstrate that although the Asp mutation of the corresponding threonine residues in hDAT and hNET similarly affects DA uptake, the Ala mutation has a differential effect on [^{3}H]DA uptake properties of hDAT and hNET. There was no significant difference in the K_m values for [^{3}H]DA uptake among hNET, T58A-hNET, and T58D-hNET (Table 1). In keeping with previous reports (Gu et al., 1994), we also observe a greater affinity for [^{3}H]DA in hNET (K_m, 0.23 μM) compared with hDAT (K_m, 2.2 μM; $p < 0.002$). The difference in K_m values for [^{3}H]DA uptake between T62A-hDAT and T58A-hNET or between T62D-hDAT and T58D-hNET were reduced or negated, demonstrating that mutation of the threonine counteracted structural differences between hDAT and hNET in affinity for [^{3}H]DA. The V_{max} for T58A-hNET, however, was more than 3 times that for T62A-hDAT ($p < 0.0001$).

TABLE 1

Kinetic properties of [^{3}H]DA uptake in hNET, hDAT, and threonine mutants K_m and V_{max} values were determined by nonlinear regression using Prism

The V_{max} values from this analysis were normalized to wild-type surface expression and are shown as mean ± S.E.M. Statistical significance was determined using Prism *F* test by comparing fits in which selected values were constrained to be equal or were allowed to differ. The null hypothesis was that the best-fit parameter for the value did not differ. A conclusion of statistical significance represents a rejection of the null hypothesis and indicates a difference between designated values. Comparison of V_{max} values within hNET: hNET vs. T58A-hNET, $P < 0.001$, $F_{1,26} = 17.21$; hNET vs. T58D-hNET, $P < 0.05$, $F_{1,26} = 5.347$. Comparison of V_{max} values within hDAT: hDAT vs. T62A-hDAT, $P < 0.01$, $F_{1,57} = 7.097$; hDAT vs. T62D-hDAT, $P < 0.05$, $F_{1,64} = 4.920$.

	V_{max}	K_m
	pmol/10^{5}cells/min	*μM*
hNET	0.76 (0.68–0.86)	0.23 (0.14–0.32)
T58A-hNET	1.3 (1.1–1.6)***	0.32 (0.10–0.53)
T58D-hNET	0.13 (0.07–0.19)*	0.12 (0.0–0.36)
hDAT[a]	0.82 (0.40–1.24)	2.2 (0.08–4.2)
T62A-hDAT[a]	0.38 (0.31–0.46)**	0.8 (0.35–1.25)
T62D-hDAT[a]	0.07 (0.052–0.094)*	0.17 (0.0–0.38)

[a] Data from Guptaroy et al. (2009).
* $P < 0.05$.
** $P < 0.01$.
*** $P < 0.001$.

Basal Efflux Is Elevated in the T58D-hNET Mutant. Because the transporter basically functions as a pump in forward and reverse transport modes, a reduction in substrate uptake (as seen in T58D-hNET) could be due to an increase in DA efflux. To evaluate this possibility for the T58D-hNET mutant, cells were loaded with [^{3}H]DA for 20 min at room temperature and rapidly washed. Efflux of [^{3}H]DA was measured every 5 min for 15 min as described under *Materials and Methods*. In Fig. 2A, basal efflux of [^{3}H]DA is expressed as percentage of the total amount of [^{3}H]DA present in the cells after the 20-min DA loading period. This representation of the data is independent of the variable surface expression because both the uptake and the efflux in each cell type depend on the number of surface transporters. The initial DA content in the cells after the loading period in units of counts per minute per 10^5 cells was: 21,649 ± 809 for hNET, 19,062 ± 486 for T58A-hNET, and 6364 ± 726 for T58D-hNET ($n = 3$). The basal efflux of [^{3}H]DA in the 5-min fraction in T58D-hNET was significantly greater than in either hNET or T58A-hNET cells (two-way ANOVA, $p < 0.001$). This efflux reached a level comparable with that of hNET and T58A-hNET by 10 min. These results suggest that the greatly reduced V_{max} of DA uptake in T58D-hNET cells is due to an increase in basal DA

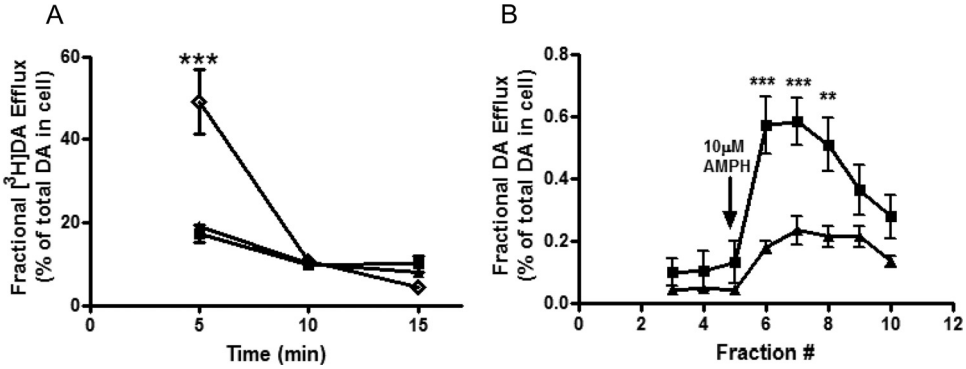

Fig. 2. Functional DA efflux properties of hNET mutants. A, cells were loaded with 5 μM [^{3}H]DA for 20 min at room temperature and washed with KRH. Basal efflux was measured in hNET (■), T58A-hNET (▲), and T58D-hNET (◇) as described under *Materials and Methods*. Efflux is expressed as the percentage of total [^{3}H]DA present in the cell at the start of the experiment ($n = 3$). In a two-way ANOVA considering time and mutants, $p < 0.001$ for time, $p < 0.01$ for mutants, and $p < 0.001$ for interaction between time and mutants. In Bonferroni post-test, ***, $p < 0.001$ for hNET or T58A-hNET compared with T58D-hNET. B, AMPH-stimulated DA efflux was assessed by superfusion of the cells as described under *Materials and Methods*. Cells were loaded with DA, washed with KRH for 30 min, and then challenged with AMPH for 2 min. Fractions (800 μl) were collected, and DA content was analyzed by high-performance liquid chromatography and electrochemical detection. Data are expressed as DA concentration in each fraction as a percentage of total amount of DA taken up in the cells ($n = 4$). In a two-way ANOVA comparing time with mutants, $p < 0.0001$ for time, $p < 0.01$ for mutants, and $p < 0.001$ for interaction between time and mutants. In Bonferroni post-test, ***, $p < 0.001$; **, $p < 0.01$.

efflux that prevents the accumulation of intracellular DA, similar to our results reported with T62D-hDAT (Guptaroy et al., 2009). For T62D-hDAT, this property was attributed to a preference for a more inward-facing conformation. In view of the similarity in characteristics of [^{3}H]DA uptake and basal [^{3}H]DA efflux between T62D-hDAT and T58D-hNET, it is reasonable to postulate that the underlying mechanism leading to this phenotype is the same in both these mutant transporters, supporting the conclusion that T58D-hNET, like T62D-hDAT, is predominantly inward-facing.

AMPH-Stimulated DA Efflux Is Reduced in T58A-hNET. AMPH-stimulated DA efflux was measured in T58A-hNET and hNET at a single AMPH concentration (10 μM) using a superfusion protocol. After loading with unlabeled DA, cells were placed in a superfusion apparatus, and DA efflux in response to 10 μM AMPH was measured. To eliminate variability due to uneven loading, data were calculated as fractional DA efflux, which is the amount of DA in the effluent as a percentage of the total amount of DA originally present in the cells. As shown in Fig. 2B, in T58A-hNET cells there was significantly less AMPH-stimulated DA efflux compared with hNET. The fact that DA influx was enhanced but the responsiveness to AMPH was reduced in T58A-hNET compared with hNET suggests that mutation of Thr58 to Ala may elicit a conformation that is slow to transition back to outward-facing. On the contrary, the T58D-hNET mutant was completely unresponsive to AMPH (data not shown). As demonstrated in the data in Fig. 2A, the baseline efflux was elevated in T58D-hNET compared with hNET and T58A-hNET, but there was no response to AMPH.

The IC_{50} for Inhibition of [^{3}H]DA Uptake by Substrates Is Decreased in Thr Mutants. Mutants with altered conformational equilibrium interact differentially with substrates and inhibitors (Chen et al., 2001, 2004b; Loland et al., 2002, 2008; Schmitt et al., 2008; Liang et al., 2009). We examined the effect of the mutations on the potency for substrates and inhibitors to functionally inhibit [^{3}H]DA uptake. As shown in Fig. 3, mutation of hNET Thr58 to Asp decreases the IC_{50} for both catechol (Fig. 3, A, DA, and B, NE) and noncatechol substrates (Fig. 3C, AMPH), as demonstrated by a leftward shift of the competition curve. Accordingly, the IC_{50} values were significantly lower for DA, NE, and AMPH in T58D-hNET compared with hNET. The IC_{50} values, 95% confidence intervals (CI), and *F*-distribution showing significant differences are given in Table 2. Mutation of Thr58 to Ala in hNET similarly increased the potency of DA and AMPH in inhibiting [^{3}H]DA uptake but not to the same extent as for the T→D mutation (T58A-hNET versus T58D-hNET for DA, $p < 0.0001$; for AMPH, $p < 0.0001$). A similar decrease in the IC_{50} of all three substrates was observed in T62D-hDAT (Fig. 3, C and D, and Table 2) compared with hDAT. As with Thr58 in hNET, mutation of Thr62 in hDAT to Ala increased the potency for DA and AMPH but not to the same degree as the T→D mutation (T62A-hDAT versus T62D-hDAT for DA, $p < 0.05$; for AMPH, $p < 0.0001$). Furthermore, the preference for AMPH over DA is lost in the T58D-hNET mutants and greatly reduced in the T62D-hDAT mutants compared with wild type. The potency of NE, however, was not significantly changed by a Thr-to-Ala mutation in either hNET or hDAT.

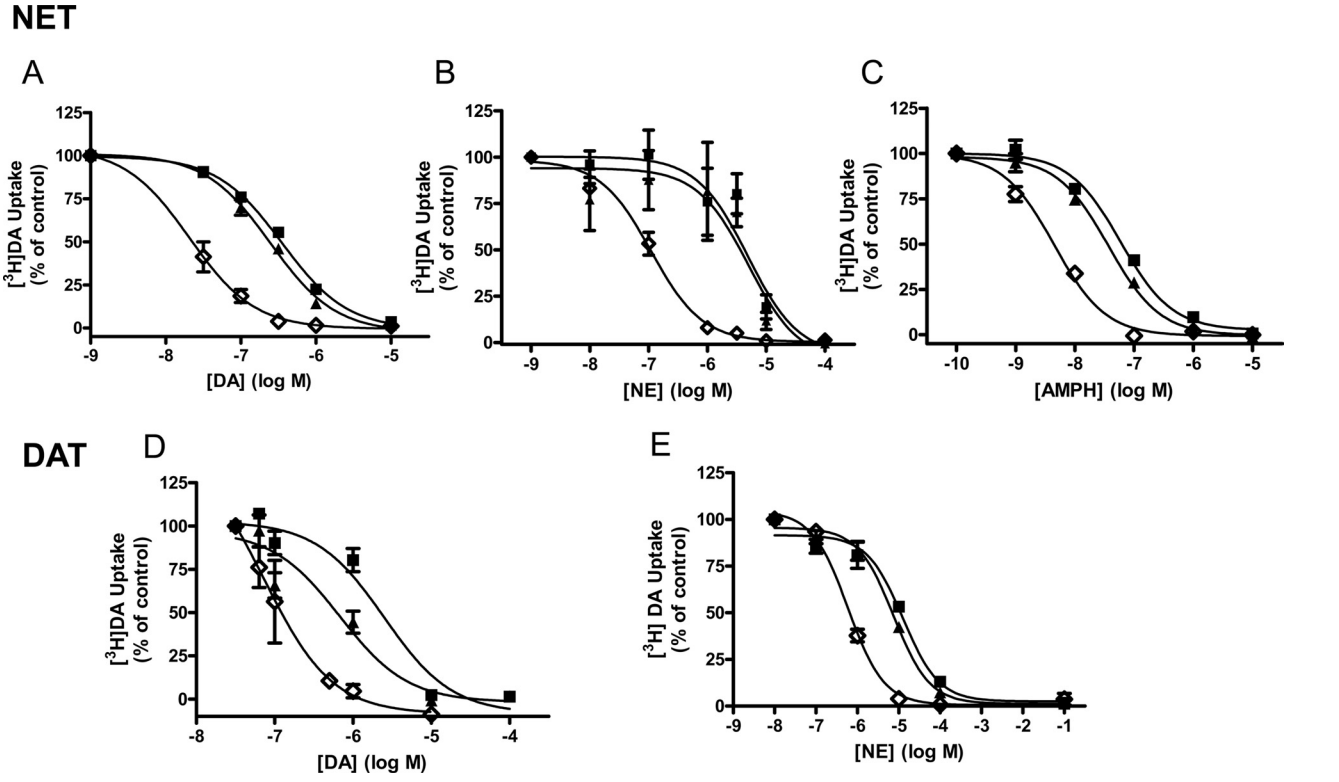

Fig. 3. Mutation of Thr58 (hNET) and Thr62 (hDAT) to aspartate results in enhanced substrate potency. DA transport was measured in hNET (■), T58A-hNET (▲), and T58D-hNET (◇) cells in the presence of increasing concentration of DA (A), NE (B), and AMPH (C) and in hDAT (■), T62A-hDAT (▲), and T62D-hDAT (◇) cells in the presence of increasing concentrations of DA (D) and NE (E). Cells were incubated with 30 nM [^{3}H]DA and indicated concentrations of competing substrate for 3 min at room temperature and processed as described under *Materials and Methods*. Data are expressed as percentage of [^{3}H]DA uptake in the absence of any added substrate (control). IC_{50} values, 95% confidence intervals, and statistical analysis of the results are given in Table 2.

In contrast to the change in IC_{50} values of substrates for DA uptake, the mutations have no effect on the sensitivity of inhibitors to block [^{3}H]DA transport in hNET mutants. IC_{50} values for cocaine, benztropine, nisoxetine, and desipramine did not significantly differ among hNET, T58A-hNET, and T58D-hNET (Table 2). On the contrary, the potency of cocaine and benztropine to inhibit [^{3}H]DA uptake was reduced in T62D-hDAT compared with hDAT. Both drugs are more selective for hDAT than for hNET. The potencies of cocaine and benztropine were reduced in T62D-hDAT compared with wild type, but they were able to completely block the [^{3}H]DA uptake. The potency of GBR12935, a highly selective DAT inhibitor of a different structural class, was unaltered by mutation of Thr62 to Asp. A Thr to Ala mutation did not change potency for any inhibitor in either hNET or hDAT. Therefore, mutation of Thr to Asp or Thr to Ala within the RETW sequence of hDAT or hNET disrupted the functional activity of the transporter substrates much more than the transporter inhibitors.

The IC_{50} values of the inhibitors for hNET reported here are higher than some reported values (Owens et al., 1997; Eshleman et al., 1999; Han and Gu, 2006) but similar to others (Mortensen and Amara, 2006). This could be attributed to differences in assay conditions and cell lines (Han and Gu, 2006). Passage number and expression level in transfected cells caused variability in the inhibition potency of cocaine for DA uptake (Chen and Reith, 2007; Ukairo et al., 2007). The use of [^{3}H]DA as opposed to [^{3}H]NE as substrate might have affected the IC_{50} values. In contrast, the IC_{50} for inhibition of binding (Tables 3 and 4) were comparable with values reported previously (Reith et al., 2005), possibly because of the similarity of the assay conditions and reagents used.

The Potency of Substrates, but Not Inhibitors, for Binding to hNET or hDAT Is Increased in Thr Mutants. To determine whether Thr58 contributes to the binding of substrates and inhibitors, we tested substrate and inhibitor competition of whole-cell [^{3}H]nisoxetine binding to NET and its mutants. When the binding assays were performed at room temperature, as were the [^{3}H]DA uptake assays, the pattern of change in potency of substrates mirrored that of the [^{3}H]DA uptake studies. There was no change in K_d for [^{3}H]nisoxetine among the three mutants. The K_d values for hNET ($n = 3$), T58A-hNET ($n = 5$), and T58D-hNET ($n = 5$) were 3.3 ± 1, 4.6 ± 0.6, and 7.0 ± 1 nM (± S.E.M.), respectively. As shown in Table 3, the potencies of DA ($p < 0.01$) and AMPH ($p < 0.02$) for T58D-hNET were significantly greater than that for hNET. There was no change in potency for NE in T62D-hNET, but there was a reduction in the number of [^{3}H]nisoxetine binding sites that the catecholamine could access. In hNET, 18% (95% CI, 7.9–27) of the total [^{3}H]nisoxetine binding sites were inaccessible to maximal concentrations of NE compared with 45% (95% CI, 34–55) of the total binding sites in T58D-hNET ($p < 0.005$, $F_{1,30} = 15.16$). There was no significant change in potency for DA or AMPH at T58A-hNET compared with hNET. As shown in the bottom panels of Table 3, there was no change in potency for any inhibitor measured, including nisoxetine, for T58A-hNET or T58D-hNET compared with hNET.

A similar result was seen with the Thr62 mutations in hDAT (Table 4). The potency for both DA ($p < 0.0001$) and AMPH ($p < 0.001$) to compete for [^{3}H]WIN35,428 binding was greatly increased in T62D-hDAT compared with hDAT. Moreover, the potency of DA ($p < 0.01$) and AMPH ($p < 0.002$) was significantly increased in T62A-hDAT compared with hDAT. These data mirror the effects of the hDAT mu-

TABLE 2

Potency for substrates and inhibitors in inhibiting [^{3}H]DA uptake in hNET and hDAT mutants

Data were calculated as a percentage of uptake in the absence of competing substrate or inhibitor and analyzed by nonlinear regression. Data displayed in the table are IC_{50} values with confidence intervals (CI) given in parentheses ($n = 3$–6). Statistical significance was determined by an F test by comparing fits in which selected values were constrained to be equal or were allowed to differ. The null hypothesis was that the best-fit parameter for the value did not differ. A conclusion of statistical significance represents a rejection of the null hypothesis and indicates a difference between designated values

	hNET	T58A-hNET	T58D-hNET	hDAT	T62A-hDAT	T62D-hDAT
			nM			
Substrates						
DA	340	230*	6***	2510	680*	54***
($n = 3$)	(280–410)	(180–300)	(2–20)	(1250–5000)	(270–1700)	(18–160)
		$F_{1,30} = 4.694$	$F_{1,30} = 206.6$		$F_{1,29} = 6.544$	$F_{1,29} = 50.77$)
NE	550	370	70***	12,600	7500	590***
($n = 3$)	(350–850)	(140–900)	(50–90)	(7900–20,000)	(5500–10,000)	(460–760)
			$F_{1,30} = 63.95$			$F_{1,30} = 128.1$
AMPH	59	37*	5***	310	130**	12***
(hNET, $n = 3$; hDAT, $n = 6$)	(43–82)	(28–48)	(3.4–5.9)	(270–350)	(120–150)	(9–17)
		$F_{1,30} = 4.80$	$F_{1,30} = 140.4$		$F_{1,30} = 11.93$	$F_{1,30} = 62.33$
Inhibitors						
Cocaine	3970	3180	6240	260	300	1130**
(hNET, $n = 3$; hDAT, $n = 6$)	(2000–7900)	(1470–6880)	(3500–11,300)	(130–510)	(180–510)	(540–2400)
						$F_{1,64} = 9.261$
Benztropine	3730	4760	9250	140	170	1240***
(hNET, $n = 3$; hDAT, $n = 6$)	(2060–6750)	(2250–10,000)	(3600–23,300)	(65–310)	(120–250)	(540–2800)
						$F_{1,64} = 19.86$
Nisoxetine	32	30	16	N.D.	N.D.	N.D.
($n = 3$)	(20–50)	(13–73)	(6–40)			
Desipramine	19	15	12	N.D.	N.D.	N.D.
($n = 3$)	(12–30)	(8–29)	(8–17)			
GBR12935	N.D.	N.D.	N.D.	105	109	191
($n = 6$)				(81–135)	(51–231)	(90–388)

* $P < 0.05$ compared with wild-type value.
** $P < 0.01$ compared with wild-type value.
*** $P < 0.001$ compared with wild-type value.

tations on inhibitory potency for [^{3}H]DA uptake, signaling that the substrate binding site is close to, if not identical with, the substrate transport site. As shown in Table 4, there was no change in potency of GBR12935 or benztropine to compete for [^{3}H]WIN35,428 binding to hDAT, T62A-hDAT, or T62D-hDAT. The K_d for hDAT, T62A-hDAT, and T62D-hDAT are 16 ± 2, 10 ± 1, and 7 ± 1 nM (± S.E.M.), respectively ($n = 3$). There was, however, an increase in potency for binding of cocaine to T62D-hDAT ($p < 0.02$), in contrast to the reduction in potency for cocaine to block [^{3}H]DA uptake.

The Potency and Extent of Substrate Binding in T58D-hNET Is Sensitive to Temperature. In some experiments, we performed [^{3}H]nisoxetine-binding assays on ice as described previously (Distelmaier et al., 2004) and found notable differences in binding characteristics when the assays were conducted at 4° versus at room temperature. The K_d values for [^{3}H]nisoxetine binding in hNET, T58A-hNET, and T58D-hNET at 4° were 4.9 ± 1, 7.6 ± 0.7, and 6.7 ± 1 nM (± S.E.M.), respectively, $n = 3$. These values were not different from each other and were not different from those measured at room temperature. The IC_{50} values for DA and NE in hNET were comparable and unchanged when measured at the two temperatures (Table 3), but the potency for AMPH was more than 60-fold greater when assayed at 4°C (3 nM) compared with room temperature (182 nM). The 95% confidence intervals and *F*-distributions for all IC_{50} values are given in Table 3. In the T58A-hNET cells, the IC_{50} values for DA and AMPH were significantly reduced at 4°C compared with RT, but there was no change in potency for NE. IC_{50} values for DA and AMPH competition of [^{3}H]nisoxetine binding in T58A-hNET cells at RT versus 4°C were for DA, 370 versus 89 nM, respectively, $p < 0.05$; for AMPH, 100 versus 5 nM, respectively, $p < 0.0001$. Striking changes in competition for [^{3}H]nisoxetine binding to T58D-hNET were noted for all substrates at the two temperatures. The potency for DA in T58D-hNET at 4°C was not significantly changed from that measured at RT, but there was a striking change in the accessibility of the [^{3}H]nisoxetine sites for which DA could compete. Access of all three substrates to all of the sites labeled with [^{3}H]nisoxetine in T58D-hNET cells was restricted (shown for AMPH in Fig. 4). DA could compete for only 30% of the [^{3}H]nisoxetine binding sites at 4°C compared with RT, and AMPH competed for only 41%. In T58D-hNET cells, the percentage unbound for DA in competing for [^{3}H]nisoxetine sites is 43% (95% CI, 25–61) at RT versus 70% at 4°C (95% CI, 65–75) ($p < 0.002$, $F_{1,24} = 12.03$). The percentage unbound for AMPH at RT is 35% (95% CI, 26–42) versus 59% (95% CI, 54–64) at 4°C ($p < 0.0001$; $F_{1,63} = 23.73$). In hNET and T58A-hNET, AMPH competed for more than 80% of the [^{3}H]nisoxetine binding sites at 4°C, demonstrating that T58D-hNET was most severely compromised at the low temperature (Fig. 4). NE was unable to compete for [^{3}H]nisoxetine binding sites in T58D-hNET at any concentration (Table 3). In contrast to the sensitivity of substrate competition for temperature, there was no change in either potency or extent of competition for [^{3}H]nisoxetine binding for the inhibitors desipramine or cocaine at RT versus 4°C.

We examined whether substrate competition for [^{3}H]WIN35,428 binding in hDAT was similarly temperature-sensitive. The K_d values for [^{3}H]WIN35,428 binding in the hDAT mutants at 4°C were not different from one another and were not different

TABLE 3

Potency for substrates and inhibitors in competing for [^{3}H]nisoxetine binding in hNET mutants

Data were calculated as a percent of total [^{3}H]nisoxetine binding in the absence of competing substrate or inhibitor and analyzed by nonlinear regression. Data displayed in the table are IC_{50} values with confidence intervals (CI) given within parenthesis. The number of experiments (n) is given under the ligand. Statistical significance was determined by an *F* test by comparing fits in which selected values were constrained to be equal or were allowed to differ. The null hypothesis was that the best fit parameter for the value did not differ. A conclusion of statistical significance represents a rejection of the null hypothesis and indicates a difference between designated values. *F* test values and degrees of freedom are given only in cases of statistical differences.

Ligands	IC_{50} (95% CI)					
	Room Temperature			4°C		
	hNET	T58A-hNET	T58D-hNET	hNET	T58A-hNET	T58D-hNET
	nM					
Substrates						
DA	490	370	35*	384	89*†	44*
($n = 3$)	(230–1000)	(140–1000)	(3–430)	(170–850)	(52–160)	(3–60)
			$F_{1,23} = 7.474$*		$F_{1,30} = 6.845$*	$F_{1,20} = 4.814$**
					$F_{1,26} = 4.958^{\dagger}$	
NE	308	745*	141	527	427	N.S.
(RT, $n = 3$)	(139–681)	(527–1051)	(28–697)	(182–1524)	(177–1031)	
(4°C, $n = 6$)		$F_{1,30} = 5.287$*				
AMPH	182	102	16*	2.7†††	4.6†††	5.3
(RT, $n = 3$)	(58–565)	(39–270)	(5.2–47)	(1.5–4.7)	(3.4–6.3)	(2.2–12)
(4°C, $n = 6$)			$F_{1,30} = 6.703$*	$F_{1,63} = 31.64^{\dagger\dagger\dagger}$	$F_{1,63} = 39.03^{\dagger\dagger\dagger}$	
Inhibitors						
Cocaine	1122	1680	1340	858	1208	1171
	(383–3280)	(793–3960)	(416–4340)	(678–1080)	(496–2943)	(200–6900)
Desipramine	10	12	6	18	12	18
	(5.9–18)	(6.2–23)	(1.2–27)	(14–23)	(9–16)	(5–67)
Benztropine	3290	4088	4990	N.D.	N.D.	N.D.
	(2280–4760)	(2626–6365)	(1848–13,480)			

N.S., no significant binding.
* $P < 0.05$ compared with wild-type value.
** $P < 0.01$ compared with wild-type value.
*** $P < 0.001$ compared with wild-type value.
† $P < 0.05$ compared with values at RT.
†† $P < 0.01$ compared with values at RT.
††† $P < 0.001$ compared with values at RT.

from those measured at room temperature. The K_d values for [^{3}H]WIN35,428 binding in hDAT, T62A-hDAT, and T62D-hDAT at 4° were 20 ± 3, 12 ± 4, and 7 ± 4 nM (± S.E.M.), respectively, $n = 3$. As shown in Table 4 and Fig. 5, the potency for DA and AMPH was increased in both hDAT and T62A-hDAT when [^{3}H]WIN35,428 binding was measured at 4°C compared with RT. The IC_{50} value for DA competition for [^{3}H]WIN35,428 binding in hDAT was 1.3 μM at RT versus 73 nM at 4°C ($p < 0.0005$) and in T62A-hDAT was 460 nM at RT versus 17 nM at 4°C ($p < 0.05$). The IC_{50} value for AMPH competition for [^{3}H]WIN35,428 binding in hDAT was 390 nM at RT versus 113 nM at 4°C ($p < 0.05$). The binding curves are shown in Fig. 5, and the 95% confidence limits and *F*-distributions for these values are given in Table 4. The potency of DA for [^{3}H]WIN35,428 binding in T62D-hDAT was already very high and was not changed at 4°C. The potency of AMPH for T62D-hDAT at 4°C is compromised by the sharply reduced accessibility of AMPH, similar to that seen with hNET. DA accessed 84% [16% unbound (95% CI, 4.7–28)] of the [^{3}H]WIN35,428 binding sites in T62D-hDAT at RT but accessed only 53% [47% unbound (95% CI, 39–55)] of the sites at 4°C ($p < 0.0001$; $F_{1,29} = 22.48$). Likewise, AMPH accessed 73% [27% unbound (95% CI, 21–33)] of the total [^{3}H]WIN35,428 binding sites in T62D-hDAT at RT but could access only 29% (95% CI, 58–84) of [^{3}H]WIN35,428 binding sites at 4°C ($p < 0.05$; $F_{1,45} = 5.158$). These data suggest that at 4°C, the transporter favors a conformation that

TABLE 4

Potency for substrates and inhibitors in competing for [^{3}H]WIN35,428 binding in hDAT mutants

Data were calculated as a percent of total [^{3}H]WIN35,428 binding in the absence of competing substrate or inhibitor and analyzed by nonlinear regression. Data displayed in the table are IC_{50} values with confidence intervals (CI) given within parenthesis. The number of experiments (n) is given under the ligand. Statistical significance was determined by an F-test by comparing fits in which selected values were constrained to be equal or were allowed to differ. The null hypothesis was that the best fit parameter for the value did not differ. A conclusion of statistical significance represents a rejection of the null hypothesis and indicates a difference between designated values. F-test values and degrees of freedom are given only in cases of statistical differences.

Ligands	IC_{50} (95% CI)					
	Room Temperature			4°C		
	hDAT	T62A-hDAT	T62D-hDAT	hDAT	T62A-hDAT	T62D-hDAT
	nM					
Substrates						
DA	1300	460**	11***	73††	17†††	10
($n = 3$)	(75–2370)	(280–760)	(3.2–43)	(24–220)	(9–34)	(2.2–49)
		$F_{1,30} = 8.176$**	$F_{1,30} = 37.92$***	$F_{1,30} = 15.21$††	$F_{1,30} = 43.45$†††	
AMPH	390	62**	8***	113†	16†	110
(RT, $n = 3$)	(200–750)	(32–120)	(4–15)	(60–220)	(6–38)	(4.9–4100)
(4°C, $n = 6$)		$F_{1,30} = 11.93$**	$F_{1,30} = 63.33$***	$F_{1,30} = 5.380$†	$F_{1,30} = 5.513$†	
AMPH + 100 μM Zn^{2+}				494‡	61‡‡	13
($n = 3$)				(260–940)	(43–88)	(3–45)
				$F_{1,30} = 7.108$‡	$F_{1,30} = 8.476$‡‡	
Inhibitors						
Cocaine	222	205	46*	N.D.	N.D.	N.D.
($n = 3$)	(120–410)	(98–430)	(16–130)			
			$F_{1,30} = 6.127$*			
Benztropine	63	99	160	N.D.	N.D.	N.D.
($n = 3$)	(38–100)	(39–253)	(100–486)			
GBR12935	50	125	113	N.D.	N.D.	N.D.
($n = 3$)	(20–130)	(56–280)	(45–290)			

N.D., not determined.
* $P < 0.05$ compared with wild-type value.
** $P < 0.01$ compared with wild-type value.
*** $P < 0.001$ compared with wild-type value.
† $P < 0.05$ compared with values at RT.
†† $P < 0.01$ compared with values at RT.
††† $P < 0.001$ compared with values at RT.
‡ $P < 0.05$ compared with values at 4°C.
‡‡ $P < 0.01$ compared with values at 4°C.

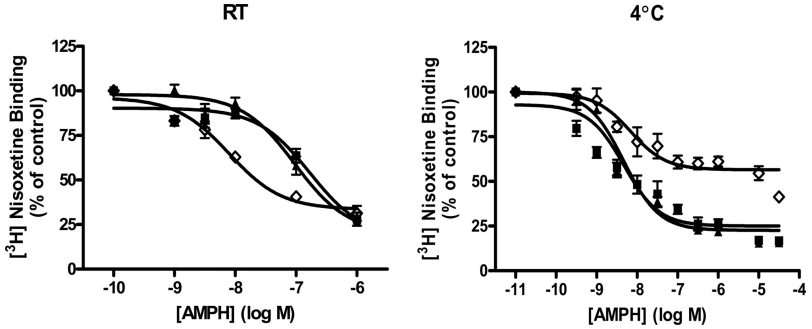

Fig. 4. At 4°C, the accessibility of AMPH to [^{3}H]nisoxetine binding sites is reduced in T58D-hNET compared with binding at room temperature (RT). hNET (■), T58A-hNET (▲), and T58D-hNET (◇) cells were incubated with 3 nM [^{3}H]nisoxetine and indicated concentrations of AMPH (0–30 μM) for 90 min at ambient temperature (RT) or 30 min at 4°C. Data (n = 3–9) are calculated as [^{3}H]nisoxetine binding in the presence of different concentrations of AMPH and expressed as a percentage of binding in the absence of AMPH (control). IC_{50} values and statistical values are given in Table 3 and text.

can readily accommodate binding of inhibitors but not substrates.

Zn^{2+} Rescues Substrate Binding at Low Temperature in T62D-hDAT. The effect of conformation on transporter activity can be examined in DAT because of its sensitivity to the ion Zn^{2+}. DAT, as opposed to NET, contains three residues in its extracellular loops that coordinately bind Zn^{2+} (Norregaard et al., 1998). Upon binding to DAT, Zn^{2+} potentiates an uncoupled Cl^- conductance in DAT, which modulates the membrane potential such that DA uptake is restricted and DA efflux is enhanced (Meinild et al., 2004). In the presence of Zn^{2+}, the equilibria of mutant transporters that seem predominantly inward-facing, in which DA uptake is compromised, are shifted toward a more outward-facing conformation, resulting in enhanced DA uptake (Loland et al., 2002; Chen et al., 2004a; Guptaroy et al., 2009). We examined whether Zn^{2+} would shift the equilibrium of substrate binding at 4°C to more resemble the potency and availability for substrates to bind at RT. As shown in Fig. 5 and Table 4, the potency of AMPH for [^{3}H]WIN35,428 binding to hDAT was increased 3-fold when assayed on ice, but when 100 μM Zn^{2+} was present at 4°C, the curve was identical to that assayed at RT. The IC_{50} for AMPH at 4°C + Zn^{2+} was 494 nM (95% CI, 26–94) compared with 113 nM (95% CI, 6–22) at 4°C ($p < 0.02$). When the T62A-hDAT mutant was measured at 4°C, there was a significant reduction in the IC_{50} for AMPH but also a significant reduction in the percentage of binding sites accessed (11% unbound at RT (95% CI, 0.8–20) versus 36% unbound at 4°C (95% CI, 31–47) ($p < 0.0004$; $F_{1,29} = 15.74$). As seen in Fig. 5B, addition of Zn^{2+} at 4°C restored the potency of AMPH in T62A-hDAT cells to RT levels [IC_{50} at 4°C + Zn^{2+}, 61 nM (95% CI, 43–88); $p < 0.01$ compared with 4°C] and enhanced the accessibility of AMPH to [^{3}H]WIN35,428 binding sites [percentage unbound at 4°C + Zn^{2+}, 19% (95% CI, 13–23) ($p < 0.002$; $F_{1,29} = 11.95$) compared with 4°C]. As shown in Fig. 5C, the dramatic reduction in the ability of AMPH to access [^{3}H]WIN35,428 in T62D-hDAT cells was corrected when 100 μM Zn^{2+} was included at 4°C. Inclusion of 100 μM Zn^{2+} in the assay significantly restored the accessibility of AMPH to [^{3}H]WIN35,428 sites (4°C + Zn^{2+}, 44% unbound; $p < 0.05$; $F_{1,46} = 4.233$). Zn^{2+} also seemed to restore the potency of AMPH to match that attained at RT, but the difference in IC_{50} values between 4°C and 4°C + Zn^{2+} [IC_{50}, 13 nM (95% CI, 3–45)] was not statistically significant because of the variability in binding at 4°C.

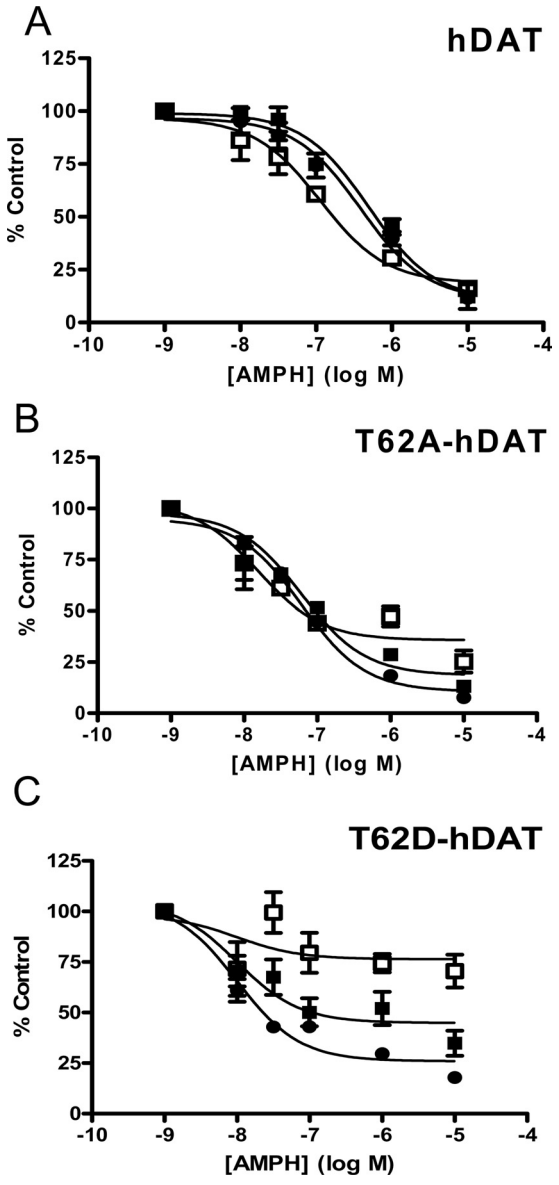

Fig. 5. Temperature-dependent changes in competition of AMPH for [^{3}H]WIN35,428 binding to hDAT mutants are reversed by addition of Zn^{2+}. The hDAT (A) T62A-hDAT (B), and T62D-hDAT (C) cells were incubated with 4 nM [^{3}H]WIN35,428 at room temperature (●), on ice (□), or on ice in the presence of 100 μM Zn^{2+} (■). Data (n = 3–9) are shown as a percentage of [^{3}H]WIN35,428 bound in the absence of any AMPH (control) at the given concentrations of AMPH (0–10 μM). IC_{50} values, bottom-of-curve values, and statistical analyses are given in Table 3 and text.

Benztropine and Cocaine Interact Differentially with T62D-hDAT. Examination of the data in Tables 2 and 3 reveal that, for assays conducted at RT, there is a strong concordance in IC_{50} values for inhibition of [^{3}H]DA uptake with the IC_{50} values obtained for competition of radioligand binding. This is true for substrates and generally true for inhibitors with the exception of the effects of cocaine and benztropine at T62D-hDAT. The IC_{50} values for cocaine and benztropine in inhibiting [^{3}H]DA uptake at T62D-hDAT were increased, showing a reduction in potency compared with hDAT (Table 2). On the other hand, this reduction in potency compared with hDAT was not exhibited when cocaine and benztropine competed for [^{3}H]WIN35,428 binding. For these drugs, there is discordance between their effectiveness in inhibiting DA uptake and their ability to bind to T62D-hDAT. This is seen clearly in Fig. 6, in which the dose-response curves for inhibition of [^{3}H]DA uptake in hDAT and T62D-hDAT are compared for those for competition with [^{3}H]WIN35,428 binding. The IC_{50} for benztropine inhibition of [^{3}H]DA in hDAT (126 nM; 95% CI, 58–271) does not differ from that of the IC_{50} for [^{3}H]WIN35,428 binding competition (65 nM; 95% CI, 35–107). On the contrary, in T62D-hDAT cells, the IC_{50} for benztropine in inhibiting [^{3}H]DA uptake (851 nM; 95% CI, 514-1411) is significantly greater than that for competition of [^{3}H]WIN35,428 binding (163 nM; 95% CI, 81–325; $p < 0.002$). Likewise, in hDAT cells, the IC_{50} for blockade of [^{3}H]DA uptake by cocaine (253 nM; 95% CI, 127–505) is the same as that for competition for [^{3}H]WIN35,428 binding (223 nM; 95% CI, 121–411). In

T62D-hDAT cells, the difference between inhibitory potency and binding potency for cocaine is greater than that for benztropine, primarily because of an enhancement in binding potency for cocaine compared with wild type. The IC_{50} for cocaine in inhibiting [^{3}H]DA uptake in T62D-hDAT cells [1130 nM (95% CI, 536-2380)] is significantly greater than the IC_{50} for competing with [^{3}H]WIN35,428 [48 nM (95% CI, 17–133); $p < 0.0001$].

Discussion

The bidirectional transport of substrates through monoamine transporters and their interaction with therapeutic and abused psychostimulant drugs is conformation-dependent. Emerging evidence indicates that interactions between specific transporter residues are critically important for maintaining relevant conformations and, when disrupted by mutations, affect transporter function. Here we show that mutations in a conserved N-terminal threonine residue of DAT and NET alter transporter conformation and function.

The juxtamembrane threonine residue (Thr62 in DAT, Thr58 in NET) resides in the RETW motif, which is a putative phosphorylation site for protein kinase C/A/G, although phosphorylation at this site has not yet been shown. We demonstrated that mutations that mimic the phosphorylation state of this threonine residue have profound effects on the conformation and function of DAT (Guptaroy et al., 2009). This intracellular threonine residue is not part of the substrate-binding site and presumably affects the permeation pathway indirectly through its effect on the interaction of critical residues. An elegant study exploring the nature of the conformational changes associated with substrate transport in $LeuT_{Aa}$ demonstrated that movement of the amino acid residue at position 7 of the N-terminal is associated with opening and closing of the inward gate (Zhao et al., 2010). In $LeuT_{Aa}$, the histidine residue at position 7 in the REHW motif corresponds to the threonine residue in RETW of DAT and NET and could potentially be critical in intracellular gating in monoamine transporters. In addition, these residues are adjacent to those involved in a conserved interaction network at the intracellular gate, which in DAT includes Val259 and Tyr335 (Kniazeff et al., 2008). Using molecular dynamic simulation, we demonstrated that mutations at Thr62 in hDAT disrupts its interaction with Lys260, which is adjacent to Val259, and consequently affects the interaction between Val259 and Tyr335 (Guptaroy et al., 2009). The greater structural disruption of the aspartate mutant compared with the alanine mutant was reflected in their functional activities. The data suggested that T62D-hDAT preferred an inward-facing conformation. We now demonstrate that corresponding mutations in NET result in similar but not identical phenotypes, although the overall conformational changes are probably similar. Differences could be due to the inherent dissimilarities between the two structures. It is suggested that both alanine and aspartate mutants of the homologous threonine residue in the serotonin, DA, and NE transporters promote an inward facing conformation and lack AMPH-stimulated efflux (Sucic et al., 2010). Though our data for the aspartate mutants in DAT and NET agree with

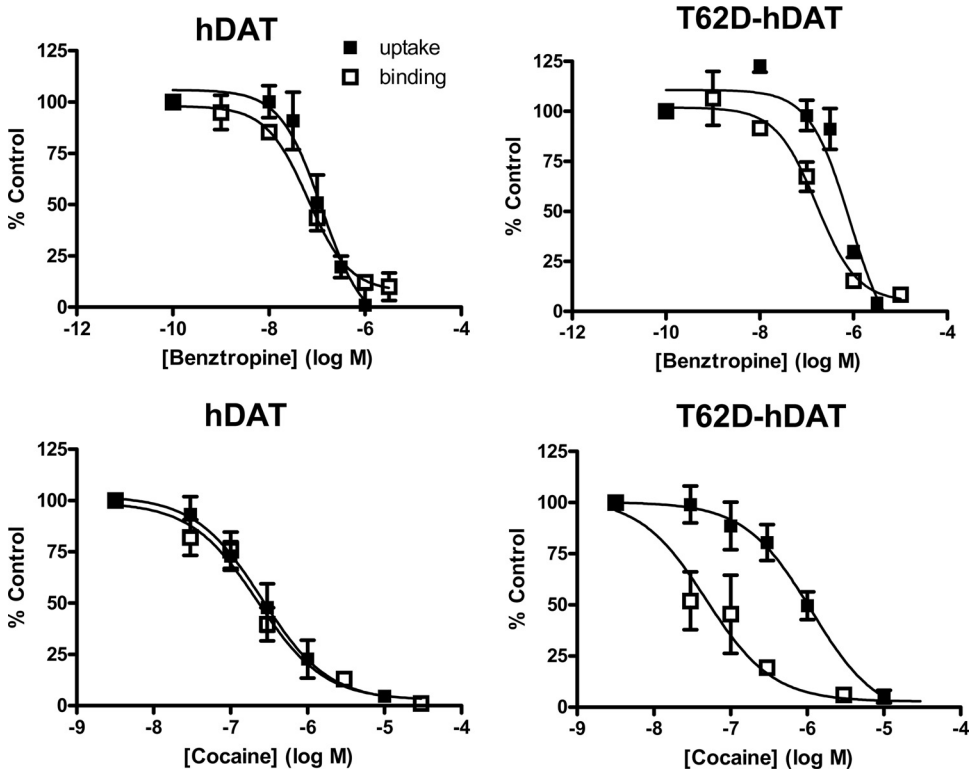

Fig. 6. Dissociation of benztropine and cocaine potencies for [^{3}H]DA uptake and competition for [^{3}H]WIN35,428 binding T62D-hDAT cells. Dose-response curves representing potency of benztropine (top) and cocaine (bottom) for inhibition of [^{3}H]DA uptake (■) and competition for [^{3}H]WIN35,428 binding (□) binding in hDAT (left) and T62D-hDAT cells (right). The assays were conducted as described under *Materials and Methods*. Data (n = 3–12) are shown as percentage of value in the absence of benztropine or cocaine (control). IC_{50} values are given in Tables 2 and 3. Statistical comparisons of IC_{50} values for inhibition of DA uptake versus [^{3}H]WIN35,428 competition in T62D-hDAT: for benztropine, $p < 0.002$, $F_{1,52} = 11.65$; for cocaine, $p < 0.0001$, $F_{1,47} = 18.33$. For both cocaine and benztropine in hDAT, $p > 0.3$.

these findings, we have consistently detected AMPH-stimulated DA efflux in the alanine mutants, although to a lesser extent than in the wild-type transporter. The reduced efflux in T58A-hNET could be due to a slow outward transition rate, resulting in a conformation that could be more inward-facing than that of hNET. However, the overall nature of interaction of substrates and inhibitors with the alanine mutants remained more similar to that of the wild-type transporter, leading us to conclude that the conformation of the alanine mutants of hDAT and hNET retains similarity to the wild-type transporter.

DA influx activity diverges between DAT and NET in the alanine mutants, although efflux properties are similar. In T62A-hDAT, both influx and AMPH-stimulated efflux of DA were reduced, and this was attributed to a slowing of the transition between the inward and outward states of the transporter (Guptaroy et al., 2009). In contrast, in T58A-hNET, we see opposing effects on DA influx (increased) and efflux (reduced). The rate of inward and outward transition might also be affected in T58A-hNET. The N-terminal domains of DAT and NET have low homology and are of dissimilar lengths, which could contribute to differences between the uptake characteristics of T62A-hDAT and T58A-hNET. The alanine mutation may affect the interaction of diverse proteins with hDAT and hNET or differentially affect the interaction with the same protein.

In both hNET and hDAT, the aspartate mutation increased the potency for DA and AMPH to inhibit [^{3}H]DA uptake and compete for radioligand binding. The alanine mutation behaved similarly, except for substrate binding in hNET. The general concordance of potency in function and binding suggests that the conformation elicited by either the Ala or Asp mutations increases the affinity for substrates at their binding site. An increase in accessibility of the substrates is unlikely because the substrate potency for transporter binding was enhanced at 4°C, but accessibility to the binding sites was often reduced. Nor is it likely that there is a defect in reorientation of the DA-transporter complex to an outward-facing form, which would kinetically result in an increased potency for substrates (Chen et al., 2004a), because basal efflux of [^{3}H]DA was enhanced in both T58D-hNET (Fig. 2A) and T62D-hDAT (Guptaroy et al., 2009). The apparent affinity for substrates was also increased in Y335A-hDAT and D345N-hDAT, which are postulated to prefer a predominantly inward-facing conformation (Chen et al., 2001, 2004a; Loland et al., 2002). Increases in functional and binding potencies were most notable for AMPH. Potency for NE was only enhanced for inhibition of [^{3}H]DA uptake in the aspartate mutants compared with wild-type transporter. Some of these disparities could result from structural variations of the substrates. Because of the benzene-diol and the α-hydroxy side chain group, NE would have more points of attachment within the binding pocket than would AMPH (Indarte et al., 2008). Fewer required attachment points for the noncatechol AMPH may permit the substrate to more easily attain an energetically favorable ligand pose within the binding pocket.

The effect of conformational restriction on substrate binding was further demonstrated by measurement of radioligand binding at 4°C. At 4°C, the conformation of hNET or hDAT was restricted into one resembling an inward-facing conformation, because the potency of substrates, especially AMPH, was significantly increased compared with RT values. The mobility of the aspartate mutants was severely compromised such that substrates could not access all [^{3}H]radioligand binding sites, but inhibitor binding was unaffected. The restoration of AMPH's access to [^{3}H]WIN35,428 binding sites in hDAT as well as the reduction of AMPH's binding potency to RT values by Zn^{2+} strongly indicates a limited mobility of an inward-facing conformation of hDAT at 4°C. Indeed, in D345N-hDAT, Zn^{2+} stimulated [^{3}H]WIN35,428 binding by countering the defect in outward reorientation of the

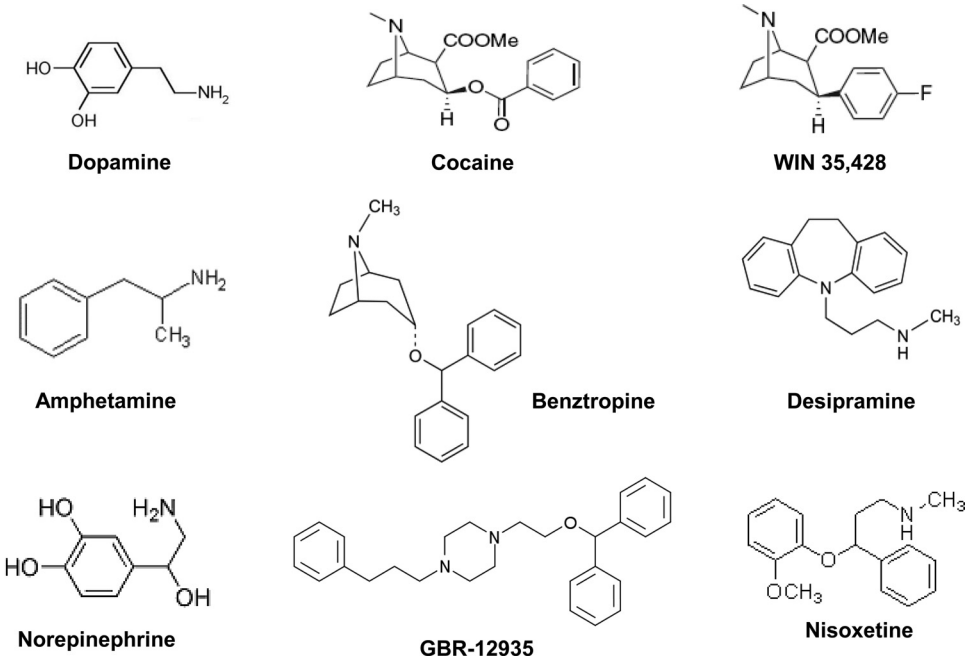

Fig. 7. Chemical structure of substrates and inhibitors. These include substrates dopamine, norepinephrine, and amphetamine and inhibitors cocaine and the cocaine analog WIN35,428, benztropine, GBR-12935, desipramine, and nisoxetine.

transporter (Chen et al., 2004a). However, a reduced potency for DA was observed at 4°C by Bonnet et al. (1990), but this study was performed in rat striatal membranes. No temperature-dependent difference was observed in the K_i for DA binding in hDAT-transfected human embryonic kidney 293 cells (Chen et al., 2001) but we saw no difference in the K_i for hNET. The reason for the increased potency for substrates at 4°C is unclear but is under investigation.

The threonine mutations affected substrates more strongly than tested inhibitors (Fig. 7), with the exception of cocaine and benztropine effects on hDAT. In particular, there was no effect of the mutations on the function or binding of desipramine or nisoxetine in hNET or on GBR12935 in hDAT. The structure of $LeuT_{Aa}$ suggests a separation in substrate and some inhibitor binding in transporter proteins (Singh, 2008). Within $LeuT_{Aa}$, a secondary binding site located extracellularly to the substrate binding site (Shi et al., 2008) serves as a vestibule for binding antidepressants (Singh et al., 2007; Zhou et al., 2007). On the basis of these results, homology-based molecular modeling identified two putative binding pockets in NET and DAT: one that binds cocaine and corresponds to the leucine binding site and another similar to the clomipramine binding site in $LeuT_{Aa}$ (Ravna et al., 2009). Interaction between residues further into the lipid bilayer in TM1 are predicted to be altered in the interaction with tricyclic antidepressants including desipramine (Henry et al., 2007) and may not be as severely affected by these threonine mutations.

The modification of the substrate binding site in the threonine mutants may account for the altered activity of benztropine and cocaine in the aspartate mutants. Molecular modeling of DAT suggests that the binding sites of DA, AMPH, cocaine, and benztropine-like drugs overlap and correspond to the substrate binding site in $LeuT_{Aa}$ that is distinct from the antidepressant binding pocket (Beuming et al., 2008). These drugs are weak inhibitors at hNET, so their binding to hNET may not have been affected by the aspartate mutation. The impaired ability of cocaine and other inhibitors to inhibit DA uptake in Y335A-DAT was attributed to its shift to an inward-facing conformation (Loland et al., 2002), and the prevailing notion that cocaine binds to and stabilizes transporters in their outward-facing conformation (Chen and Justice, 1998; Loland et al., 2004). Other inward-facing mutants of hDAT (D345N, D436A, and K264A) show similar but less dramatic decreases in the inhibitory potency of cocaine (Chen et al., 2004a; Loland et al., 2004). Our data suggest that cocaine and benztropine bind normally to T62D-hDAT but have a reduced potency in inhibiting DA uptake. There is, therefore, discordance between inhibitor radioligand binding and function. A lack of correlation has been observed previously in cocaine potency for inhibition of uptake and binding in wild-type DAT (Wang et al., 2003). It cannot be excluded that disruption of the normal translocation cycle in mutants transporters causes uptake and binding affinities to diverge. These results support the notion that the DAT conformation responsible for inhibitor high-affinity binding is less responsible for DA uptake (Wang et al., 2003). In some DAT mutants, cocaine, and benztropine interactions differ (Chen et al., 2004b; Ukairo et al., 2005; Loland et al., 2008; Schmitt et al., 2008). Because both cocaine and benztropine compounds contain tropane rings, the altered conformation of T62D-hDAT may affect side-chain associations with this ring structure. It is unclear why the binding potency of cocaine is increased in T62D-hDAT. It could be that T62D-hDAT rapidly oscillates between inward and outward states—a condition supported by its enhanced basal efflux, which is contingent upon the transporter more readily assuming an outward conformation.

The above evidence strongly argues for a critical role of the highly conserved threonine residue in the juxtamembrane N-terminal domain of monoamine transporters in determining transporter conformation and functions such as substrate binding, permeation, reverse transport, and drug interactions.

Acknowledgments

We thank Dr. Randy D. Blakely (Vanderbilt University, Nashville, TN) for providing hNET cDNA and Dr. Jonathan A. Javitch (Columbia University, New York, NY) for the FLAG-hDAT cDNA. Benztropine was generously provided by Dr. A. K. Dutta (Wayne State University, Detroit, MI). We thank Dr. Rick Neubig for helpful conversations concerning the kinetics of radioligand binding. We thank Hobart Ng Ng Tsai for technical assistance.

Authorship Contributions

Participated in research design: Guptaroy, Fraser, and Gnegy.
Conducted experiments: Guptaroy, Fraser, Zhang, and Desai.
Contributed new reagents or analytic tools: Guptaroy.
Performed data analysis: Guptaroy, Fraser, and Gnegy.
Wrote or contributed to the writing of the manuscript: Guptaroy and Gnegy.
Other: Gnegy acquired funding for the research.

References

Amara SG and Kuhar MJ (1993) Neurotransmitter transporters: recent progress. *Annu Rev Neurosci* **16:**73–93.
Bennett ER, Su H, and Kanner BI (2000) Mutation of arginine 44 of GAT-1, a (Na^+ + Cl^-)-coupled gamma-aminobutyric acid transporter from rat brain, impairs net flux but not exchange. *J Biol Chem* **275:**34106–34113.
Beuming T, Kniazeff J, Bergmann ML, Shi L, Gracia L, Raniszewska K, Newman AH, Javitch JA, Weinstein H, Gether U, et al. (2008) The binding sites for cocaine and dopamine in the dopamine transporter overlap. *Nat Neurosci* **11:**780–789.
Blakely RD and Bauman AL (2000) Biogenic amine transporters: regulation in flux. *Curr Opin Neurobiol* **10:**328–336.
Bonnet JJ, Benmansour S, Costentin J, Parker EM, and Cubeddu LX (1990) Thermodynamic analyses of the binding of substrates and uptake inhibitors on the neuronal carrier of dopamine labeled with [^{3}H]GBR 12783 or [^{3}H]mazindol. *J Pharmacol Exp Ther* **253:**1206–1214.
Chen N and Justice JB, Jr. (1998) Cocaine acts as an apparent competitive inhibitor at the outward-facing conformation of the human norepinephrine transporter: kinetic analysis of inward and outward transport. *J Neurosci* **18:**10257–10268.
Chen N and Reith ME (2000) Structure and function of the dopamine transporter. *Eur J Pharmacol* **405:**329–339.
Chen N and Reith ME (2007) Substrates and inhibitors display different sensitivity to expression level of the dopamine transporter in heterologously expressing cells. *J Neurochem* **101:**377–388.
Chen N, Rickey J, Berfield JL, and Reith ME (2004a) Aspartate 345 of the dopamine transporter is critical for conformational changes in substrate translocation and cocaine binding. *J Biol Chem* **279:**5508–5519.
Chen N, Vaughan RA, and Reith ME (2001) The role of conserved tryptophan and acidic residues in the human dopamine transporter as characterized by site-directed mutagenesis. *J Neurochem* **77:**1116–1127.
Chen N, Zhen J, and Reith ME (2004b) Mutation of Trp84 and Asp313 of the dopamine transporter reveals similar mode of binding interaction for GBR12909 and benztropine as opposed to cocaine. *J Neurochem* **89:**853–864.
Danek Burgess KS and Justice JB, Jr. (1999) Effects of serine mutations in transmembrane domain 7 of the human norepinephrine transporter on substrate binding and transport. *J Neurochem* **73:**656–664.
Distelmaier F, Wiedemann P, Brüss M, and Bönisch H (2004) Functional importance of the C-terminus of the human norepinephrine transporter. *J Neurochem* **91:**537–546.
Eshleman AJ, Carmolli M, Cumbay M, Martens CR, Neve KA, and Janowsky A (1999) Characteristics of drug interactions with recombinant biogenic amine transporters expressed in the same cell type. *J Pharmacol Exp Ther* **289:**877–885.
Giros B and Caron MG (1993) Molecular characterization of the dopamine transporter. *Trends Pharmacol Sci* **14:**43–49.
Gu H, Wall SC, and Rudnick G (1994) Stable expression of biogenic amine transporters reveals differences in inhibitor sensitivity, kinetics, and ion dependence. *J Biol Chem* **269:**7124–7130.

Guptaroy B, Zhang M, Bowton E, Binda F, Shi L, Weinstein H, Galli A, Javitch JA, Neubig RR, and Gnegy ME (2009) A juxtamembrane mutation in the N terminus of the dopamine transporter induces preference for an inward-facing conformation. *Mol Pharmacol* **75:**514–524.

Han DD and Gu HH (2006) Comparison of the monoamine transporters from human and mouse in their sensitivities to psychostimulant drugs. *BMC Pharmacol* **6:**6.

Henry LK, Meiler J, and Blakely RD (2007) Bound to be different: neurotransmitter transporters meet their bacterial cousins. *Mol Interv* **7:**306–309.

Indarte M, Madura JD, and Surratt CK (2008) Dopamine transporter comparative molecular modeling and binding site prediction using the LeuT(Aa) leucine transporter as a template. *Proteins* **70:**1033–1046.

Johnson LA, Furman CA, Zhang M, Guptaroy B, and Gnegy ME (2005) Rapid delivery of the dopamine transporter to the plasmalemmal membrane upon amphetamine stimulation. *Neuropharmacology* **49:**750–758.

Kantor L, Hewlett GH, Park YH, Richardson-Burns SM, Mellon MJ, and Gnegy ME (2001) Protein kinase C and intracellular calcium are required for amphetamine-mediated dopamine release via the norepinephrine transporter in undifferentiated PC12 cells. *J Pharmacol Exp Ther* **297:**1016–1024.

Kniazeff J, Shi L, Loland CJ, Javitch JA, Weinstein H, and Gether U (2008) An intracellular interaction network regulates conformational transitions in the dopamine transporter. *J Biol Chem* **283:**17691–17701.

Liang YJ, Zhen J, Chen N, and Reith ME (2009) Interaction of catechol and non-catechol substrates with externally or internally facing dopamine transporters. *J Neurochem* **109:**981–994.

Loland CJ, Desai RI, Zou MF, Cao J, Grundt P, Gerstbrein K, Sitte HH, Newman AH, Katz JL, and Gether U (2008) Relationship between conformational changes in the dopamine transporter and cocaine-like subjective effects of uptake inhibitors. *Mol Pharmacol* **73:**813–823.

Loland CJ, Gråsäs C, Javitch JA, and Gether U (2004) Identification of intracellular residues in the dopamine transporter critical for regulation of transporter conformation and cocaine binding. *J Biol Chem* **279:**3228–3238.

Loland CJ, Norregaard L, Litman T, and Gether U (2002) Generation of an activating Zn^{2+} switch in the dopamine transporter: mutation of an intracellular tyrosine constitutively alters the conformational equilibrium of the transport cycle. *Proc Natl Acad Sci USA* **99:**1683–1688.

Meinild AK, Sitte HH, and Gether U (2004) Zinc potentiates an uncoupled anion conductance associated with the dopamine transporter. *J Biol Chem* **279:**49671–49679.

Mortensen OV and Amara SG (2006) Gain of function mutants reveal sites important for the interaction of the atypical inhibitors benztropine and bupropion with monoamine transporters. *J Neurochem* **98:**1531–1540.

Norregaard L, Frederiksen D, Nielsen EO, and Gether U (1998) Delineation of an endogenous zinc-binding site in the human dopamine transporter. *EMBO J* **17:**4266–4273.

Norregaard L and Gether U (2001) The monoamine neurotransmitter transporters: structure, conformational changes and molecular gating. *Curr Opin Drug Discov Devel* **4:**591–601.

Owens MJ, Morgan WN, Plott SJ, and Nemeroff CB (1997) Neurotransmitter receptor and transporter binding profile of antidepressants and their metabolites. *J Pharmacol Exp Ther* **283:**1305–1322.

Ravna AW, Sylte I, and Dahl SG (2009) Structure and localisation of drug binding sites on neurotransmitter transporters. *J Mol Model* **15:**1155–1164.

Reith ME, Wang LC, and Dutta AK (2005) Pharmacological profile of radioligand binding to the norepinephrine transporter: instances of poor indication of functional activity. *J Neurosci Methods* **143:**87–94.

Rudnick G (1997) Mechanism of biogenic amine neurotransmitter transporters, in *Neurotransmitter Transporetrs: Structure, Function and Regulation* (Reith ME ed), New Jersey.

Schmitt KC, Zhen J, Kharkar P, Mishra M, Chen N, Dutta AK, and Reith ME (2008) Interaction of cocaine-, benztropine-, and GBR12909-like compounds with wild-type and mutant human dopamine transporters: molecular features that differentially determine antagonist-binding properties. *J Neurochem* **107:**928–940.

Shi L, Quick M, Zhao Y, Weinstein H, and Javitch JA (2008) The mechanism of a neurotransmitter:sodium symporter–inward release of Na^+ and substrate is triggered by substrate in a second binding site. *Mol Cell* **30:**667–677.

Singh SK (2008) LeuT: a prokaryotic stepping stone on the way to a eukaryotic neurotransmitter transporter structure. *Channels* (*Austin*) **2:**380–389.

Singh SK, Yamashita A, and Gouaux E (2007) Antidepressant binding site in a bacterial homologue of neurotransmitter transporters. *Nature* **448:**952–956.

Sucic S, Dallinger S, Zdrazil B, Weissensteiner R, Jørgensen TN, Holy M, Kudlacek O, Seidel S, Cha JH, Gether U, et al. (2010) The N terminus of monoamine transporters is a lever required for the action of amphetamines. *J Biol Chem* **285:**10924–10938.

Torres GE, Gainetdinov RR, and Caron MG (2003) Plasma membrane monoamine transporters: structure, regulation and function. *Nat Rev Neurosci* **4:**13–25.

Ukairo OT, Bondi CD, Newman AH, Kulkarni SS, Kozikowski AP, Pan S, and Surratt CK (2005) Recognition of benztropine by the dopamine transporter (DAT) differs from that of the classical dopamine uptake inhibitors cocaine, methylphenidate, and mazindol as a function of a DAT transmembrane 1 aspartic acid residue. *J Pharmacol Exp Ther* **314:**575–583.

Ukairo OT, Ramanujapuram S, and Surratt CK (2007) Fluctuation of the dopamine uptake inhibition potency of cocaine, but not amphetamine, at mammalian cells expressing the dopamine transporter. *Brain Res* **1131:**68–76.

Wang W, Sonders MS, Ukairo OT, Scott H, Kloetzel MK, and Surratt CK (2003) Dissociation of high-affinity cocaine analog binding and dopamine uptake inhibition at the dopamine transporter. *Mol Pharmacol* **64:**430–439.

Yamashita A, Singh SK, Kawate T, Jin Y, and Gouaux E (2005) Crystal structure of a bacterial homologue of Na^+/Cl^--dependent neurotransmitter transporters. *Nature* **437:**215–223.

Zhao Y, Terry D, Shi L, Weinstein H, Blanchard SC, and Javitch JA (2010) Single-molecule dynamics of gating in a neurotransmitter transporter homologue. *Nature* **465:**188–193.

Zhou Z, Zhen J, Karpowich NK, Goetz RM, Law CJ, Reith ME, and Wang DN (2007) LeuT-desipramine structure reveals how antidepressants block neurotransmitter reuptake. *Science* **317:**1390–1393.

Address correspondence to: Margaret E. Gnegy, Department of Pharmacology, 2220E MSRBIII, University of Michigan Medical School, 1150 West Medical Center Drive, Ann Arbor, MI 48109-0632. E-mail: pgnegy@umich.edu